J. Astrophys. Astr. (2011) **32,** 173–178

Ten Years of Monitoring 3C 273 with XMM–Newton

Liu Liu* & Youhong Zhang**
Department of Physics and Tsinghua Center for Astrophysics, Tsinghua University, Beijing, 100084, China.
**e-mail: liuliu08@mails.tsinghua.edu.cn*
***e-mail: youhong.zhang@mails.thu.edu.cn*

Abstract. We present ten years optical/UV/X-ray observations of 3C 273 performed using XMM–Newton between 2000 and 2009. The short-time scale variability behaviour of the soft and hard X-ray light curves may suggest different origins of the soft/hard X-ray emissions. We fit well the 0.2–10 keV X-ray spectrum with a hard power-law component plus a soft Comptonization component. The lack of Γ–F correlation of the hard power-law component and the weakness of iron K_α lines may support dominance of the jet component. The soft X-ray excess correlates much better with ultraviolet than with the hard power-law component, strongly suggesting that soft excess emission originates from inverse Comptonization of UV photons.

Key words. Quasars: individual (3C 273)—X-rays: galaxies—ultraviolet: galaxies.

1. Introduction

As one of the brightest, nearest ($z = 0.158$) and the first found radio-loud quasar, 3C 273 is characterized by both the blazar-like and the Seyfert-like emission features: the hard X-ray power-law spectrum extending to the MeV region, the optical/UV bump, and the significant soft X-ray excess. Grandi & Palumbo (2004), decoupled the X-ray emission with beamed nonthermal (jet) and unbeamed Seyfert-like components. Page *et al.* (2004) explained the soft excess as inverse Comptonization of UV photons by low temperature corona electrons. In this paper, we analyse the 10 years XMM–Newton optical/UV/X-ray observation data (2000–2009), and try to go deep into the study of the source by investigating the spectral variability of the hard X-rays, the soft X-ray excess and the optical/UV bump.

2. Short time-scale light curve

The light curves in Fig. 1, showing distinct variability trends in different energy bands, imply that the soft and hard X-ray components may be emitted by a physically distinct radiation process. Light curves in Obs. 7, with a monotonic variation of the hard X-ray component, may be explained as an increased hard component diluted by a stable soft component.

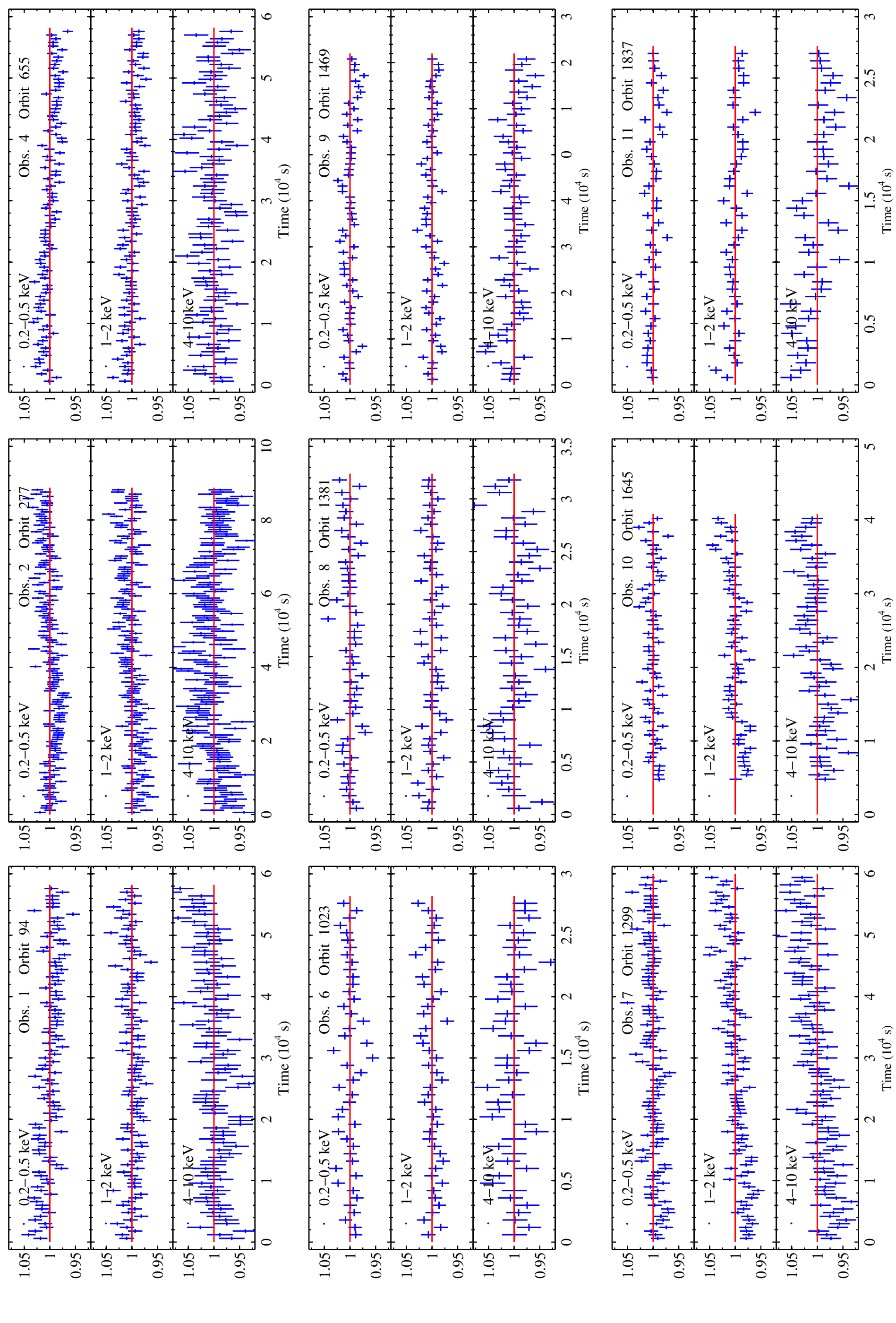
Obs. 1 Orbit 94
Obs. 2 Orbit 277
Obs. 4 Orbit 655
Obs. 6 Orbit 1023
Obs. 8 Orbit 1381
Obs. 9 Orbit 1469
Obs. 7 Orbit 1299
Obs. 10 Orbit 1645
Obs. 11 Orbit 1837
0.2–0.5 keV
1–2 keV
4–10 keV
Time (10^4 s)

3. The hard X-ray spectra and iron lines

Figure 2 plots the hard power-law photon index Γ versus flux in the 3–10 keV power-law fitting. The Spearman correlation $R = -0.58$ with a probability of random coincidence $P = 0.061$ suggests that plausible (pseudo) anti-correlation is most likely to arise from the sparse XMM–Newton observations. We add a Gaussian line component near 6.7 keV (in the quasar frame) to the 3–10 keV power-law fitting. Iron lines are only detectable in three observations at 99% confidence level (Fig. 3).

The absence of the photon index-flux correlation on the ten years XMM–Newton observations, may suggest that most of the hard X-ray continuum generally originates from the jet component. The Doppler-boosted jet emission hides the possible underlying emission of the Seyfert component. The iron lines, with equivalent width ∼30 eV, are rather weak compared to that of Seyfert 1 galaxies. Only in some short periods can the Seyfert component emerge over the jet, by showing the iron lines.

4. Soft X-ray excess

We fit the soft excess with the simplest Comptonization model in Xspec: COMPST, Comptonization of cooler seed photons by thermal electrons in hot corona (Sunyaev & Titarchuk 1980). The electron temperature T_e varies between ∼0.28 and ∼0.54 keV, and the optical depth τ changes between ∼19 and ∼26. Neither the T_e nor τ shows correlation with the soft excess flux.

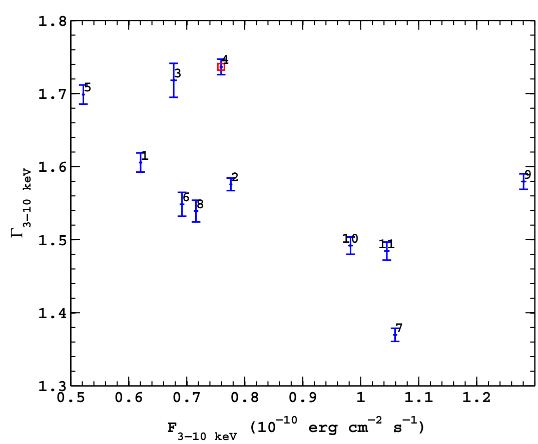

Figure 2. 3–10 keV photon index Γ versus flux. The red square denotes the observation with most significant iron line.

Figure 1. The 600 s binned background-subtracted 0.2–0.5, 1–2 and 4–10 keV normalized light curves for the nine long-exposed observations. The light curves are normalized to its mean count rates. The three rows of the plots correspond to three types of variation. Top row: different variability trend in soft and hard bands. Middle row: fluctuation in both soft and hard domain. Bottom row: larger variability amplitude in hard X-rays than in soft X-rays.

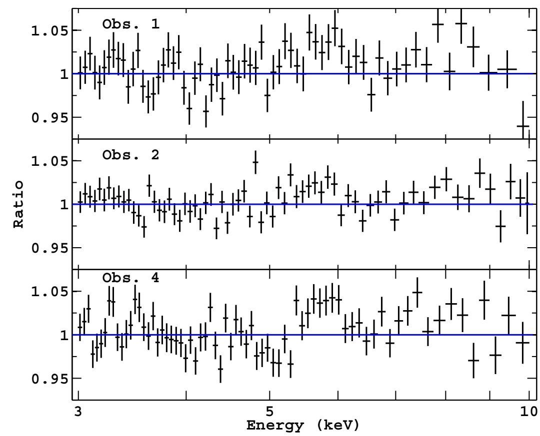

Figure 3. Three observations, showing small residuals around 5.7 keV (observer frame), indicate weak iron lines.

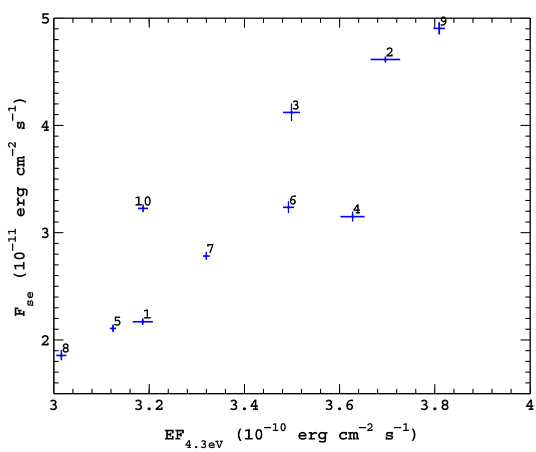

Figure 4. A good flux correlation between UV and Comptonization soft excess.

Figure 4 shows the UV flux against the soft excess flux. The Spearman correlation coefficient is 0.90, with a probability of random coincidence 8.8×10^{-4}. On the other hand, Fig. 5 plots the flux of the soft excess and the hard power-law but has poor correlation. The above comparison supports the soft excess as inverse Comptonization of UV photons.

5. The spectral energy distribution

Figure 6 plots the optical/UV/X-ray SEDs. A remarkable feature of the X-ray SEDs is the concave around 1 keV. The optical/UV bump clearly presents in the figure. The variability amplitude is larger in ultraviolet than in optical. The source shows a bluer-when-brighter feature in ultraviolet.

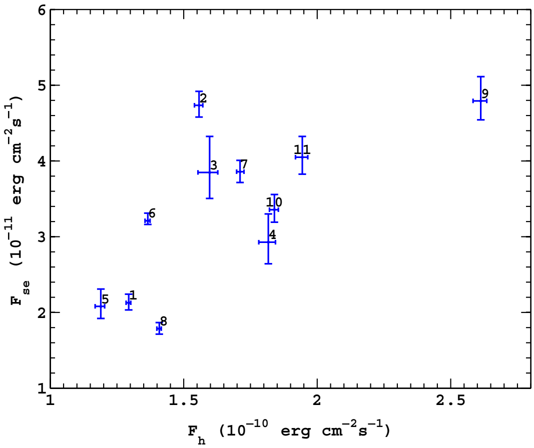

Figure 5. The soft excess flux versus the hard power-law component flux.

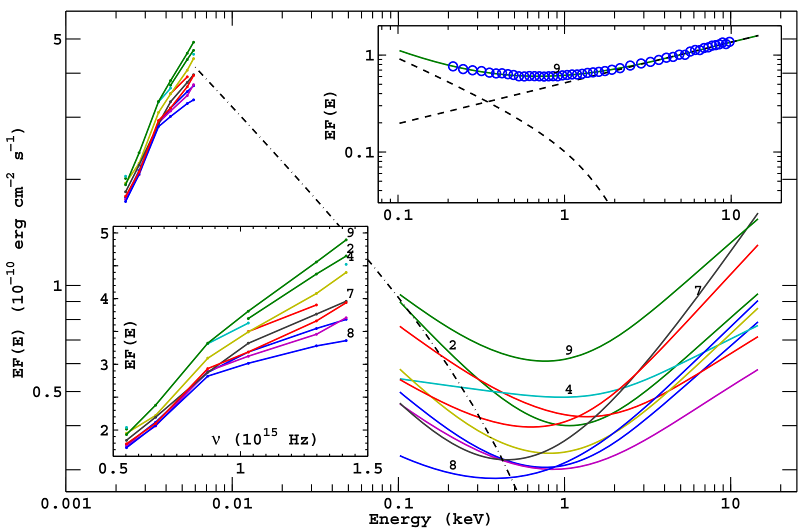

Figure 6. Optical/UV and X-ray SEDs for 10 observations. The background curves show the global view of SEDs. The dash-dotted line represents the extrapolation of the Comptonization component to the UV region as an example. The top inset shows as an example for the broad soft excess and the hard power-law components (dashed lines). Crosses are for absorption corrected observation data. The bottom inset amplifies the optical/UV SEDs for clarity. The UV variability amplitude, though larger than the optical one, is smaller than that of the soft excess. Serial numbers attached to the SED curves mark the selected observations among the total 10 observations.

6. Conclusion

We find independent variability in the soft and hard X-ray light curves. The hard X-ray emission tends to be dominated by the jet component, and the soft excess is most likely due to inverse Comptonization of UV photons.

References

Grandi, P., Palumbo, G. G. C. 2004, *Science*, **306**, 998.

Page, K. L., Turner, M. J. L., Done, C., O'Brien, P. T., Reeves, J. N., Sembay, S., Stuhlinger M. 2004, *Mon. Not. R. Astron. Soc.*, **349**, 57.

Sunyaev, R. A., Titarchuk, L. G. 1980, *Astron. Astrophys.*, **86**, 121.